

Merged contact layer in adhesion mechanics

Nikita Tsybin*

Moscow State University of Civil Engineering, 129337, Moscow, Russia

Abstract. Predicting bond strength is the most common task in adhesion mechanics. To solve these problems, a contact layer model which describes the interaction of the substrate and adhesive layers, can be used. With the use of this model, which provides calculating the inhomogeneous stress-strain state of adhesive joints, a wide range of problems has been solved. Despite the fact that solutions, as a rule, are obtained in a closed analytical form, their use for processing experimental data can be difficult due to its complexity. In this regard a method that makes it possible to reduce the order of the resolving system of equations by introducing an integral contact layer connecting the adhesive layer and adjacent contact layers is proposed in this work. The application of this approach is demonstrated by the example of the most common adhesive lapped joint. As a result, the formulas for determining the parameters of the integral contact layer have been obtained. Comparison of the results obtained for the exact solution of the problem with the results obtained for the models with an integral contact layer is carried out.

1 Problem statement

The classical problem of adhesive mechanics about the stress state of two layers of a substrate, glued with an overlap with an adhesive layer, is considered. It is assumed that the layers' interaction is carried out using a contact layer [1], which characterizes the adhesive interaction intensity. The contact layer is an orthotropic medium in which the intermolecular interaction of the adhesive and the substrate takes place. The parameters of this medium are such that it can be represented as a set of short elastic rods, unconnected with each other and oriented normally to the contact plane. As a result, the contact layer transfers shear stresses in the contact plane and normal stresses perpendicular to the contact plane. The hypotheses applied to the adhesive and substrate layers are not limited. This approach gives an opportunity to avoid infinite tangential stresses [13, 14] at the corner points (which arise in a rigorous solution of the problem under the assumption of absolute contact between the layers of the adhesive and the substrate), as well as to satisfy all boundary conditions. In [9, 10] the infinite shear stresses at corner points are eliminated due to the elastoplastic work of the adhesive. A more detailed description of the contact layer can be found in [1-3].

* Corresponding author: science@nikitatsybin.ru

It should be noted that the contact layer can be considered as an interaction layer not only between the adhesive and the substrate, but also between any two media. In [4, 5], for example, a contact layer appears at the interface between two concrete layers.

From the point of view of the contact layer model classical approach, this structure is five-layer (substrate - contact layer - adhesive - contact layer - substrate). This model is shown in Figure 1 (left). In most practically important cases, the thickness and stiffness of the adhesive layer is small compared to the thickness and stiffness of the substrate layers to be bonded. In this case, it is proposed to combine the adhesive layer and adjacent contact layers into one integral contact layer. Thus, the model becomes three-layer (substrate - integral contact layer - substrate). A three-layer model with an integral contact layer is shown in Figure 1 (right). It is assumed that bending effect is insignificant and can be neglected. The width of the layers is taken equal to one.

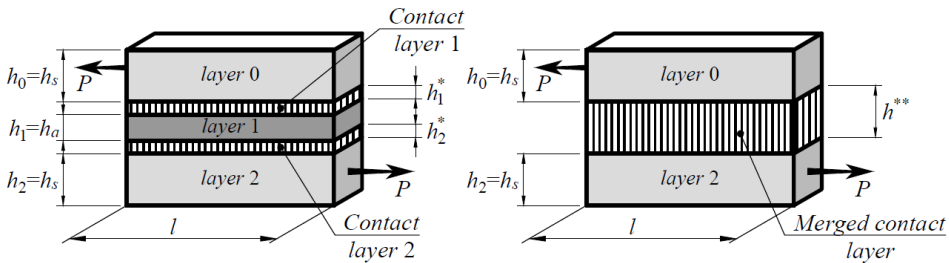


Fig. 1. Lapped joint model. Left - the classic approach from the point of view of the contact layer model. On the right is a model with a merged contact layer.

The purpose of this work is to establish a relationship between the geometric and physical and mechanical characteristics of the integral contact layer and the original layers.

2 Original system of equations

The system of resolving equations for the contact layer obtained in [6] is given below.

$$\left. \begin{aligned} u_k^* &= \frac{y_k^*}{12G_k^*} \left[(y_k^*)^2 - \frac{(h_k^*)^2}{4} \right] \frac{d^2 \tau_k^*}{dx^2} + \frac{y_k^*}{h_k^*} (u_k - u_{k-1}) + \frac{1}{2} (u_k + u_{k-1}); \\ \frac{(h_k^*)^2}{24G_k^*} \frac{d^2 \tau_k^*}{dx^2} - \frac{\tau_k^*}{G_k^*} + \frac{1}{h_k^*} (u_k - u_{k-1}) &= 0. \end{aligned} \right\} \quad (1)$$

Hereinafter, all quantities related to the contact layer will be marked with the symbol *.

The quantities are included in (1):

k is a contact layer serial number;

h_k^* is contact layer thickness;

G_k^* denotes shear stiffness of the contact layer;

y_k^* is an own axis of the contact layer, $-h_k^*/2 \leq y_k^* \leq h_k^*/2$;

u_k^* shows the displacement in the contact layer;

u_k shows the displacement in the adjoining bottom layer;

u_{k-1} shows the displacements in the adjoining top layer;

τ_k^* defines shear stresses in the contact layer.

The main parameters of the contact layer G_k^* and h_k^* are determined from a macro experiment for a specific adhesive-substrate pair. The examples of calculating these parameters can be found in the works [7, 8].

The use of the equations (1) makes it possible to fully satisfy the boundary conditions (equality to zero of tangential stresses) at the ends of the contact layer. In this case, the shear stresses reach the maximum value at some distance from the end of the model. In this case, a pronounced edge effect takes place.

In many cases, it is advisable to use a simplified model of the contact layer. In this case, due to the small thickness of the contact layer, a linear distribution of displacements over the thickness is assumed. As a result, the expressions (1) take the form:

$$\left. \begin{aligned} u_k^* &= \frac{y_k^*}{h_k^*} (u_k - u_{k-1}) + \frac{1}{2} (u_k + u_{k-1}); \\ -\frac{\tau_k^*}{G_k^*} + \frac{1}{h_k^*} (u_k - u_{k-1}) &= 0. \end{aligned} \right\} \quad (2)$$

When using the equations (2), it is not possible to satisfy the boundary conditions at the ends of the contact layer. The tangential stresses at the ends will have a finite value. The edge effect, as in the case of equations (1), is present. In [11], a comparison of the calculation results using the equations (1) and (2) is given. It should be borne in mind that use of the equations (2) greatly simplifies the resolving system of equations and makes it possible to unambiguously determine the point with the maximum value of shear stresses.

Let us consider the main layer k . In view of the bending neglect, the main layers experience a uniaxial stress-strain state. The adjoining contact layers in accordance with the section method are replaced by the shear stresses arising in them. From the equilibrium condition of the layer as a whole, we obtain:

$$\frac{dN_k}{dx} + \tau_{k+1}^* - \tau_k^* = 0. \quad (3)$$

Longitudinal force N_k is related to displacements by the ratio

$$N_k = B_k \frac{du_k}{dx}, \quad (4)$$

B_k is tensile stiffness of the layer, $B_k = E_k h_k$.

The thickness and modulus of the substrate layers' elasticity are assumed to be the same $h_0 = h_2 = h_s$, $E_0 = E_2 = E_s$. As a result:

$B_s = B_0 = B_2 = E_s h_s$ – tensile stiffness of the substrate layer;

$B_a = B_1 = E_a h_a$ – tensile stiffness of the adhesive layer.

In the future, the tensile stiffness of the adhesive layer is more convenient to be expressed through the stiffness of the substrate layer $B_a = \psi B_s$.

The final system of resolving equations is represented by the second equation (1) (in the case of a simplified model, the second equation of system (2)) and the equation (3), into

which it is necessary to substitute $k = 1, 2 \dots m$ for the contact layers and $k = 0, 1 \dots m$ for the base layers (adhesive and substrate). The displacements are expressed in terms of the longitudinal force by the ratio (4).

3 Governing equations and boundary conditions

Further in the work, 4 the models, a brief description of which is given below, will be considered.

Model 1a. Five-layer model with three main layers and two contact layers, shown in Figure 1 on the left. The equations (1) are used for the contact layers. Contact layers are the same, $h_1^* = h_2^* = h^*$, $G_1^* = G_2^* = G^*$.

Model 2a. A three-layer model with two main layers and one merged contact layer, shown in Figure 1 on the right. The equations (1) are used for the contact layer.

Model 1b. Five-layer model with three main layers and two contact layers. For the contact layers, simplified equations (2) are used. The contact layers are the same.

Model 2b. Three-layer model with two main layers and one merged contact layer. For the contact layer, the simplified equations (2) are used.

Thus, the following classification of models has been adopted: the number means the number of layers: 1 - five-layer model with two contact layers and an adhesive layer; 2 - three-layer model with an integral contact layer. The letter denotes the equations used for the contact layer: a - model with nonlinear distribution of displacements (1) along the height of the contact layer; b - model with linear distribution of displacements (2) along the height of the contact layer.

Each system of equations obtained from expressions (1), (2), and (4) can be reduced to one resolving equation for the function N_0 (longitudinal force in the upper layer of the substrate). Let us write them down without detailed conclusions.

Model 1a.

$$\begin{aligned} & \frac{d^8 N_0^{1a}}{dx^8} - 2a_1 \frac{d^6 N_0^{1a}}{dx^6} + \left[2a_1 a_2 \left(\frac{1}{\psi} + 1 \right) + a_1^2 \right] \frac{d^4 N_0^{1a}}{dx^4} - \\ & - 2a_1^2 a_2 \left(\frac{1}{\psi} + 1 \right) \frac{d^2 N_0^{1a}}{dx^2} + 2a_1^2 a_2^2 \left(\frac{1}{\psi} + \frac{1}{2} \right) N_0^{1a} - \frac{a_1^2 a_2^2}{\psi} P = 0, \\ & a_1 = \frac{24}{h^*}; \quad a_2 = \frac{G^*}{h^* B_s}; \quad \psi = \frac{B_a}{B_s}. \end{aligned} \tag{5}$$

From the solution of the equation (5), the longitudinal force in the upper layer of the substrate (layer 0) is determined.

$$\begin{aligned} N_0^{1a} = & \frac{P}{2 + \psi} + C_1^{1a} \exp(-s_1^{1a} x) + C_2^{1a} \exp(s_1^{1a} x) + C_3^{1a} \exp(-s_2^{1a} x) + C_4^{1a} \exp(s_2^{1a} x) + \\ & + C_5^{1a} \exp(-s_3^{1a} x) + C_6^{1a} \exp(s_3^{1a} x) + C_7^{1a} \exp(-s_4^{1a} x) + C_8^{1a} \exp(s_4^{1a} x). \end{aligned} \tag{6}$$

Superscript $1a$ here and below indicates the model under consideration. The roots of the characteristic equation are written below.

$$s_{1,2}^{1a} = \sqrt{\frac{a_1}{2} \pm \frac{1}{2} \sqrt{a_1(a_1 - 4a_2)}}; \quad s_{3,4}^{1a} = \sqrt{\frac{a_1}{2} \pm \frac{1}{2} \sqrt{a_1 \left[a_1 - 8a_2 \left(\frac{1}{\psi} + \frac{1}{2} \right) \right]}}. \quad (7)$$

The longitudinal force in the adhesive layer (layer 1) is related to the longitudinal force in the upper layer of the substrate by the ratio:

$$N_1^{1a} = \frac{\psi}{a_1 a_2} \frac{d^4 N_0^{1a}}{dx^4} - \frac{\psi}{a_2} \frac{d^2 N_0^{1a}}{dx^2} + \psi N_0^{1a}. \quad (8)$$

Knowing the longitudinal force in the upper substrate layer and the adhesive layer, it is possible to find the longitudinal force in the lower substrate layer (layer 2) from the conditions of static equilibrium.

$$N_2^{1a,1b} = P - N_0^{1a,1b} - N_1^{1a,1b}. \quad (9)$$

From the expressions (6), (8), (9) it is possible to determine the tangential stresses in the contact layers.

$$\tau_1^{*1a,1b} = -\frac{dN_0^{1a,1b}}{dx}; \quad \tau_2^{*1a,1b} = \frac{dN_2^{1a,1b}}{dx}. \quad (10)$$

Boundary conditions for the model 1a.

$$\left. \begin{aligned} N_0^{1a}(-l/2) = P; \quad N_0^{1a}(l/2) = 0; \quad N_1^{1a}(-l/2) = 0; \quad N_1^{1a}(l/2) = 0; \\ \tau_1^{*1a}(-l/2) = 0; \quad \tau_1^{*1a}(l/2) = 0; \quad \tau_2^{*1a}(-l/2) = 0; \quad \tau_2^{*1a}(l/2) = 0. \end{aligned} \right\} \quad (11)$$

Model 2a.

$$\frac{d^4 N_0^{2a}}{dx^4} - b_1 \frac{d^2 N_0^{2a}}{dx^2} + 2b_1 b_2 N_0^{2a} - b_1 b_2 P = 0, \quad (12)$$

$$b_1 = \frac{24}{h^{**}}; \quad b_2 = \frac{G^{**}}{h^{**} B_s}; \quad h^{**} = 2h^* + h_a,$$

h^{**} denotes the thickness of the integral contact layer. From geometric considerations, this value is taken equal to the sum of the adhesive layer and adjacent contact layers' thicknesses;

G^{**} is shear stiffness of the integral contact layer. The calculation of this value is the purpose of the work.

Below is the solution to the equation (12).

$$N_0^{2a} = \frac{P}{2} + C_1^{2a} \exp(-s_1^{2a} x) + C_2^{2a} \exp(s_1^{2a} x) + C_3^{2a} \exp(-s_2^{2a} x) + C_4^{2a} \exp(s_2^{2a} x), \quad (13)$$

in which the roots of the characteristic equation are determined by the expression:

$$s_{1,2}^{2a} = \sqrt{\frac{b_1}{2} \pm \frac{1}{2} \sqrt{b_1(b_1 - 8b_2)}}.$$

The longitudinal force in layer 2 can be found from the static equilibrium conditions.

$$N_2^{2a,2b} = P - N_0^{2a,2b}. \tag{14}$$

The shear stresses in the integral contact layer can be determined further.

$$\tau^{**2a,2b} = -\frac{dN_0^{2a,2b}}{dx} = \frac{dN_2^{2a,2b}}{dx}. \tag{15}$$

Boundary conditions for the model 2a.

$$N_0^{2a}(-l/2) = P; \quad N_0^{2a}(l/2) = 0; \quad \tau^{**2a}(-l/2) = 0; \quad \tau^{**2a}(l/2) = 0. \tag{16}$$

A distinctive feature of models 1a and 2a is the strict satisfaction of the boundary conditions and the end of the model (equality to zero of shear stresses). Due to the presence of the edge effect of shear stresses, it is not possible to explicitly determine the point with the maximum value. In this regard, it is difficult to determine the parameters of the integral contact layer from these solutions. Therefore, we consider further models 1b and 2b in which the shear stresses reach their maximum value at the end.

Model 1b.

Resolving equation for the function N_0 has the form:

$$\frac{d^4 N_0^{1b}}{dx^4} - 2a_2 \left(\frac{1}{\psi} + 1 \right) \frac{d^2 N_0^{1b}}{dx^2} + 2a_2^2 \left(\frac{1}{\psi} + \frac{1}{2} \right) N_0^{1b} - \frac{a_2^2}{\psi} P = 0. \tag{17}$$

The expressions for a_2 and ψ had been written earlier. From the equation (17) we find

$$N_0^{1b} = \frac{P}{2 + \psi} + C_1^{1b} \exp(-s_1^{1b} x) + C_2^{1b} \exp(s_1^{1b} x) + C_3^{1b} \exp(-s_2^{1b} x) + C_4^{1b} \exp(s_2^{1b} x). \tag{18}$$

Below are the roots of the characteristic equation.

$$s_1^{1b} = \sqrt{a_2}; \quad s_2^{1b} = \sqrt{2a_2 \left(\frac{1}{\psi} + \frac{1}{2} \right)}.$$

Next, we find the longitudinal force in layer 1

$$N_1^{1b} = -\frac{\psi}{a_2} \frac{d^2 N_0^{1b}}{dx^2} + \psi N_0^{1b}. \tag{19}$$

The longitudinal force in layer 2, as well as shear stresses in the contact layers, are calculated from the expressions (9) and (10).

Boundary conditions for model 1b.

$$N_0^{1b}(-l/2) = P; N_0^{1b}(l/2) = 0; N_1^{1b}(-l/2) = 0; N_1^{1b}(l/2) = 0. \tag{20}$$

Model 2b.

For model 2b, the following resolving equation is obtained for the longitudinal force in layer 0.

$$\frac{d^2 N_0^{2b}}{dx^2} - 2b_2 N_0^{2b} + b_2 P = 0. \tag{21}$$

The expression for b_2 v.

$$N_0^{2b} = \frac{P}{2} + C_1^{2b} \exp(-s_1^{2b} x) + C_2^{2b} \exp(s_1^{2b} x), \tag{22}$$

s_1^{2b} is the root of the characteristic equation, $s_1^{2b} = \sqrt{2b_2}$.

The longitudinal force in layer 2, as well as the shear stresses in the integral contact layer, are calculated from the expressions (14) and (15).

Boundary conditions for model 2b.

$$N_0^{2b}(-l/2) = P; N_0^{2b}(l/2) = 0. \tag{23}$$

The integration determination constants in the expressions (6), (13), (18), and (22) for the given boundary conditions (11), (16), (20) and (23) is not difficult. Due to their cumbersomeness, they are not presented here.

From the analysis of the obtained solutions for all considered models, it follows that the intensity of the adhesive interaction (rigidity and thickness of the contact layer) has a significant effect on the stress-strain state.

4 Calculation of the integral contact layer stiffness

As mentioned earlier, in models 1a and 2a, it is difficult to determine the point with the maximum value of shear stresses. In this regard, we will calculate the stiffness of the integral contact layer by comparing models 1b and 2b, in which the shear stresses reach their maximum value at the ends.

When determining the stiffness of the integral contact layer, we will rely on the shear stresses maximum value equality. This choice is justified by the fact that in experiments on testing the lapped joints, the main strength criterion is set on the average value of shear stresses.

From the conditions of static equilibrium, it follows:

$$P = \int_{-l/2}^{l/2} \tau_1^{*1b} dx = \int_{-l/2}^{l/2} \tau_2^{*1b} dx = \int_{-l/2}^{l/2} \tau^{**2b} dx. \tag{24}$$

It should be noted that with a low stiffness and thickness of the adhesive layer, in comparison with the substrate layers, the shear stresses τ_1^{*1b} and τ_2^{*1b} differ slightly. This fact follows from relation (3), since in this case the longitudinal force in the adhesive layer

(layer 1) will be negligible compared to the longitudinal forces in the substrate layers (layers 0 and 2). The difference between the shear stresses in contact layer 1 and contact layer 2 on the left edge of the joint for model 1b is determined by the relation:

$$\Delta\tau^{*1b} = \frac{P\psi s_2^{1b}}{2 + \psi} \cdot \frac{\cosh(s_2^{1b}l) + \sinh(s_2^{1b}l) - 1}{\cosh(s_2^{1b}l) + \sinh(s_2^{1b}l) + 1}.$$

To determine the maximum value of shear stresses in the contact layer for model 2b, the equality written below is used.

$$\tau_{\max}^{**2b} = \tau^{**2b}\left(\frac{l}{2}\right) = \frac{Ps_1^{2b}}{2} \cdot \frac{\cosh(s_1^{2b}l) + \sinh(s_1^{2b}l) + 1}{\cosh(s_1^{2b}l) + \sinh(s_1^{2b}l) - 1}.$$

Analyzing (24), we obtain the equation for calculating the parameters of the integral contact layer.

$$\tau_{\max}^{**2b} = \frac{1}{2} \left[\tau_1^{*1b}\left(\frac{l}{2}\right) + \tau_2^{*1b}\left(\frac{l}{2}\right) \right]. \tag{25}$$

From the solution (25) we find the integral contact layer rigidity

$$G^{**} = G^* \left(1 + \frac{h_a}{2h^*} \right) \tag{26}$$

Formula (26) is valid only for a small thickness and stiffness of the adhesive layer. To estimate the error in calculating the maximum value of shear stresses when using a model with an integral contact layer, the formula is used:

$$\delta\tau = \frac{\Delta\tau^{*1b}}{\tau_{\max}^{**2b}}.$$

5 Calculation example

The calculation results for the following parameters are presented as an example:

$$E_s = 7 \cdot 10^4 \text{ MPa}; E_a = 200 \text{ MPa}; h_s = 4 \text{ mm}; h_a = 0.25 \text{ mm};$$

$$l = 20 \text{ mm}; G^* = 10^3 \text{ MPa}; h^* = 0.1 \text{ mm}.$$

Below are the graphs of the shear stresses distribution in the considered models for the selected parameters.

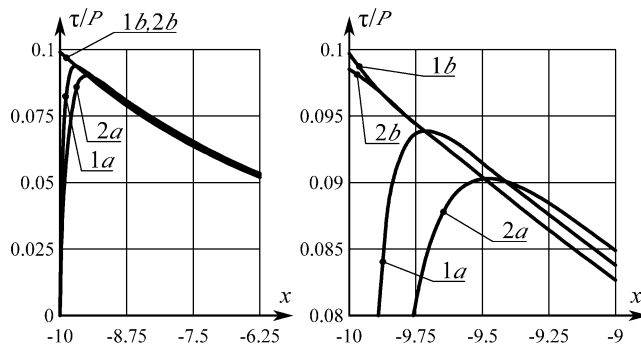


Fig. 2. Distribution of shear stresses at the gluing boundary near the end of the model. The figure captions correspond to the model under consideration.

It follows from the results obtained that the models that do not take into account the nonlinearity of the distribution of displacements over the thickness of the contact layer (1b and 2b) give overestimated results for the maximum shear stresses magnitude. In this case, the width of the edge effect zone is practically the same.

To determine the parameters of adhesive interaction with strict regulation of the thickness of the adhesive layer, it is necessary to rely on models 1a and 1b. Using model 1b, according to the experimental data of measuring the average adhesive strength, depending on the length of the overlap [12], the ratio is determined G^*/h^* and a preliminary value of the true adhesion strength τ_{ad} (maximum value of shear stresses at the model failure moment). Then, using models 1a, the value of the true adhesive τ_{ad} strength and finally determined by the rigidity G^* and the thickness of the contact layer h^* , at a given value G^*/h^* .

If the parameters of the adhesive interaction (intensity and true adhesive strength) are known for a given adhesive-substrate pair, then it is recommended to use models 2a and 2b to calculate the stress-strain state of a particular joint. The calculation using model 2b will give a certain margin of safety, since the strength criteria for such joints, as a rule, are set in the form $\tau \leq \tau_{ad}$.

The main distinguishing feature of the results obtained is that the shear stresses at the end of the model are not infinite.

6 Conclusion

The article provides the solutions for calculating overlap adhesive joints. Fig. 2 shows that the maximum shear stresses are at the end of the joint, and not in the middle of its length. Moreover, the distribution is essentially nonlinear. From the analysis of the obtained solutions, it follows that the rigidity and thickness of the contact layer (the intensity of the adhesive interaction) has a significant effect on the nature and values of the stress-strain state components. As a result, it can be concluded that the average adhesive strength alone is insufficient to characterize the adhesive interaction.

The approach proposed in this article to reduce the order of the resolving system of equations by introducing an integral contact layer does not introduce a significant error in the calculation results for the models with a linear distribution of displacements over the thickness of the contact layer (curves 1b and 2b in Fig. 2). For the models that take into account the nonlinearity of the displacements' distribution over the contact layer thickness

(curves 1a and 2a in Fig. 2), the error is larger. From this it follows that the formula for determining the stiffness of the integral contact layer (26) for such models can be refined in further studies.

References

1. R. Turusov, Adhesion mechanics (NRU MGSU, 2015)
2. V. Andreev, R. Turusov, N. Tsybin, Procedia Engineering **153**, (2016)
3. V. Andreev, N. Tsybin, R. Turusov, E3S Web of Conferences **97**, 04071 (2019)
4. V. Tho, E. Korol, Vestnik MGSU **15** (7), (2020)
5. E. Korol, V. Tho, N. Hoang, MATEC Web of Conferences **196**, 02022 (2018)
6. R. Turusov, V. Andreev, N. Tsybin, IOP Conf. Series: Materials Science and Engineering **913**, 032053 (2020)
7. A. Sergeev, R. Turusov, V. Andreev, IOP Conf. Series: Materials Science and Engineering **1030**, 012001 (2021)
8. R. Turusov, L. Manevich, Polymer science. Series D **3**(2), 75 (2010)
9. V. Glagolev, A. Markin, Mechanics of Solids **55**(6), 837 (2020)
10. V. Glagolev, A. Markin, A. Fursaev, PNRPU Mechanics Bulletin **1**, (2018)
11. V. Andreev, R. Turusov, N. Tsybin, MATEC Web of Conferences **251**, 04066 (2018)
12. E. Lertora, D. Campanella, C. Mandolfino, C. Gambaro, L. Fratini, G. Buffa, AIP Conference Proceedings **1896** (1), 110004 (2017)
13. Y. Wang, Y. Li, K. Zhou, Advances in Materials Science and Engineering **1**, (2018)
14. A. Chiminelli, R. Breto, S. Izquierdo, L. Bergamasco, E. Duviolier, M. Lizaranzu, International Journal of Adhesion and Adhesives **76**, (2017)